NeuroImage 130 (2016) 24–34

Contents lists available at ScienceDirect

NeuroImage

journal homepage: www.elsevier.com/locate/ynimg

Limited microstructural and connectivity deficits despite subcortical volume reductions in school-aged children born preterm with very low birth weight

Anne Elisabeth Sølsnes [a,1], Kam Sripada [a,*,1], Anastasia Yendiki [b], Knut Jørgen Bjuland [a], Heidi Furre Østgård [a], Synne Aanes [a], Kristine Hermansen Grunewaldt [a,c], Gro C. Løhaugen [a,d], Live Eikenes [e], Asta K. Håberg [e,f,g], Lars M. Rimol [a], Jon Skranes [a,d]

[a] Department of Laboratory Medicine, Children's and Women's Health, Norwegian University of Science and Technology, Trondheim, Norway
[b] Department of Radiology, Athinoula A. Martinos Center for Biomedical Imaging, Massachusetts General Hospital and Harvard Medical School, Boston, MA, USA
[c] Department of Pediatrics, St. Olav's Hospital, Trondheim, Norway
[d] Department of Pediatrics, Sørlandet Hospital, Arendal, Norway
[e] Department of Circulation and Medical Imaging, Norwegian University of Science and Technology, Trondheim, Norway
[f] Department of Neuroscience, Norwegian University of Science and Technology, Trondheim, Norway
[g] Department of Medical Imaging, St. Olav's Hospital, Trondheim, Norway

ARTICLE INFO

Article history:
Received 31 August 2015
Accepted 16 December 2015
Available online 20 December 2015

Keywords:
DTI
Cohort study
Connectivity
Tractography
Premature
Development

ABSTRACT

Preterm birth and very low birth weight (VLBW, ≤1500 g) are worldwide problems that burden survivors with lifelong cognitive, psychological, and physical challenges. In this multimodal structural magnetic resonance imaging (MRI) and diffusion MRI (dMRI) study, we investigated differences in subcortical brain volumes and white matter tract properties in children born preterm with VLBW compared to term-born controls (mean age = 8 years). Subcortical brain structure volumes and cortical thickness estimates were obtained, and fractional anisotropy (FA), mean diffusivity (MD), radial diffusivity (RD), and axial diffusivity (AD) were generated for 18 white matter tracts. We also assessed structural relationships between white matter tracts and cortical thickness of the tract endpoints. Compared to controls, the VLBW group had reduced volumes of thalamus, globus pallidus, corpus callosum, cerebral white matter, ventral diencephalon, and brain stem, while the ventricular system was larger in VLBW subjects, after controlling for age, sex, IQ, and estimated total intracranial volume. For the dMRI parameters, group differences were not significant at the whole-tract level, though pointwise analysis found shorter segments affected in forceps minor and left superior longitudinal fasciculus – temporal bundle. IQ did not correlate with subcortical volumes or dMRI measures in the VLBW group. While the deviations in subcortical volumes were substantial, there were few differences in dMRI measures between the two groups, which may reflect the influence of advances in perinatal care on white matter development.

Introduction

Preterm birth (gestational age < 37 weeks) is a worldwide problem, affecting 15 million newborns each year and burdening many survivors with lifelong cognitive, psychological, and physical challenges (Chang et al., 2013; Lawn et al., 2014; Saigal and Doyle, 2008). Advances in perinatal care, including the introduction of surfactant therapy for preterm infants, led to improved survival rates starting in the 1990s (Wilson-Costello et al., 2005). While survival rates have improved and prevalence of severe focal brain injuries, including intraventricular hemorrhages grades III and IV and cystic periventricular leukomalacia, has decreased, adverse long-term neurological outcomes are common in preterm-born individuals (Ferriero, 2004; Back et al., 2007). Low IQ and poorer attention/executive functions and academic outcomes have frequently been associated with very low birth weight (VLBW, birth weight ≤ 1500 g) and preterm birth (Løhaugen et al., 2010; Aarnoudse-Moens et al., 2009; Lund et al., 2012). Diffuse white matter injury including axonal abnormalities and gliosis is considered the dominant neuropathology in preterm-born infants and is believed to underlie many of these cognitive and sensorimotor deficits (Volpe et al., 2011; Haynes et al., 2011).

White matter near the lateral ventricles and in centrum semiovale has long been known to be especially vulnerable to perinatal injury

* Corresponding author at: Department of Laboratory Medicine, Children's and Women's Health, Medical Faculty, Norwegian University of Science and Technology, 7489 Trondheim, Norway.
E-mail address: kam.sripada@ntnu.no (K. Sripada).
[1] Shared first authorship.

http://dx.doi.org/10.1016/j.neuroimage.2015.12.029

among preterm-born individuals (Banker and Larroche, 1962), and hypoxia-ischemia and inflammation are considered the underlying causes behind periventricular white matter injury in preterms (Ortinau and Neil, 2015). Diffusion magnetic resonance imaging (dMRI), which measures Brownian motion of water diffusion of white matter bundles in the brain (Le Bihan and Johansen-Berg, 2012; Johansen-Berg and Behrens, 2014), has been used to identify white matter tracts that appear particularly sensitive to the effects of preterm birth and VLBW, such as corpus callosum and long-range association tracts (Counsell et al., 2008; Constable et al., 2008; Skranes et al., 2007; Eikenes et al., 2011; Ment et al., 2009; Mento and Bisiacchi, 2012; Hintz and O'Shea, 2008).

In line with the widely reported "encephalopathy of prematurity" of diffuse white matter injury and tissue loss typical among preterms, deviations in volumes of subcortical structures have also been reported in the VLBW population (Volpe, 2009; Boardman et al., 2010). Cerebral white matter, thalamus, globus pallidus, nucleus accumbens, and corpus callosum volumes may be vulnerable to neonatal risk factors such as VLBW (Bjuland et al., 2014). Deep gray matter abnormalities have been found in tandem with diffuse white matter injury among infants (Boardman et al., 2006), toddlers (Lowe et al., 2011), and school-aged children (Murray et al., 2014).

In a recent paper (Sølsnes et al., 2015), we reported significant differences in cortical architecture in our cohort of term-born controls recruited from the Norwegian Mother and Child Cohort Study and VLBW children born between 2001 and 2007, with increased cortical thickness frontally and occipitally, and reduced cortical surface area in widespread regions in the VLBW group, consistent with previous reports from year cohorts of VLBW teenagers born in 1986–88 (Skranes et al., 2007, 2013; Eikenes et al., 2011; Bjuland et al., 2013; Martinussen et al., 2005). It is not known whether these cortical deviations are secondary to the reported abnormalities in white matter tracts connected to these cortical regions or represent primary cortical injury.

This study therefore aimed to investigate subcortical volumes, white matter properties, and possible relationships between white matter tracts and the cortical changes previously reported in the same cohort of school-aged children. We explored group differences in fractional anisotropy and diffusivity using TRACULA, a novel tool for automated reconstruction of 18 major white matter tracts, as well as subcortical structure volumes using FreeSurfer. Moreover, we assessed structural relationships between white matter tracts of interest and cortical thickness of the tract endpoints. We also investigated possible relationships between neuroimaging findings and full-scale IQ scores and perinatal risk factors.

Methods

Participants

VLBW group

Preterm-born VLBW subjects (birth weight ≤ 1500 g), born between 2003 and 2007, were recruited based on admittance to the Neonatal Intensive Care Unit at St. Olav's University Hospital in Trondheim, Norway. Sixty-three children were invited and 57 agreed to participate in the study (Fig. 1). Age ranged from 5.0 to 10.5 years old (mean age =

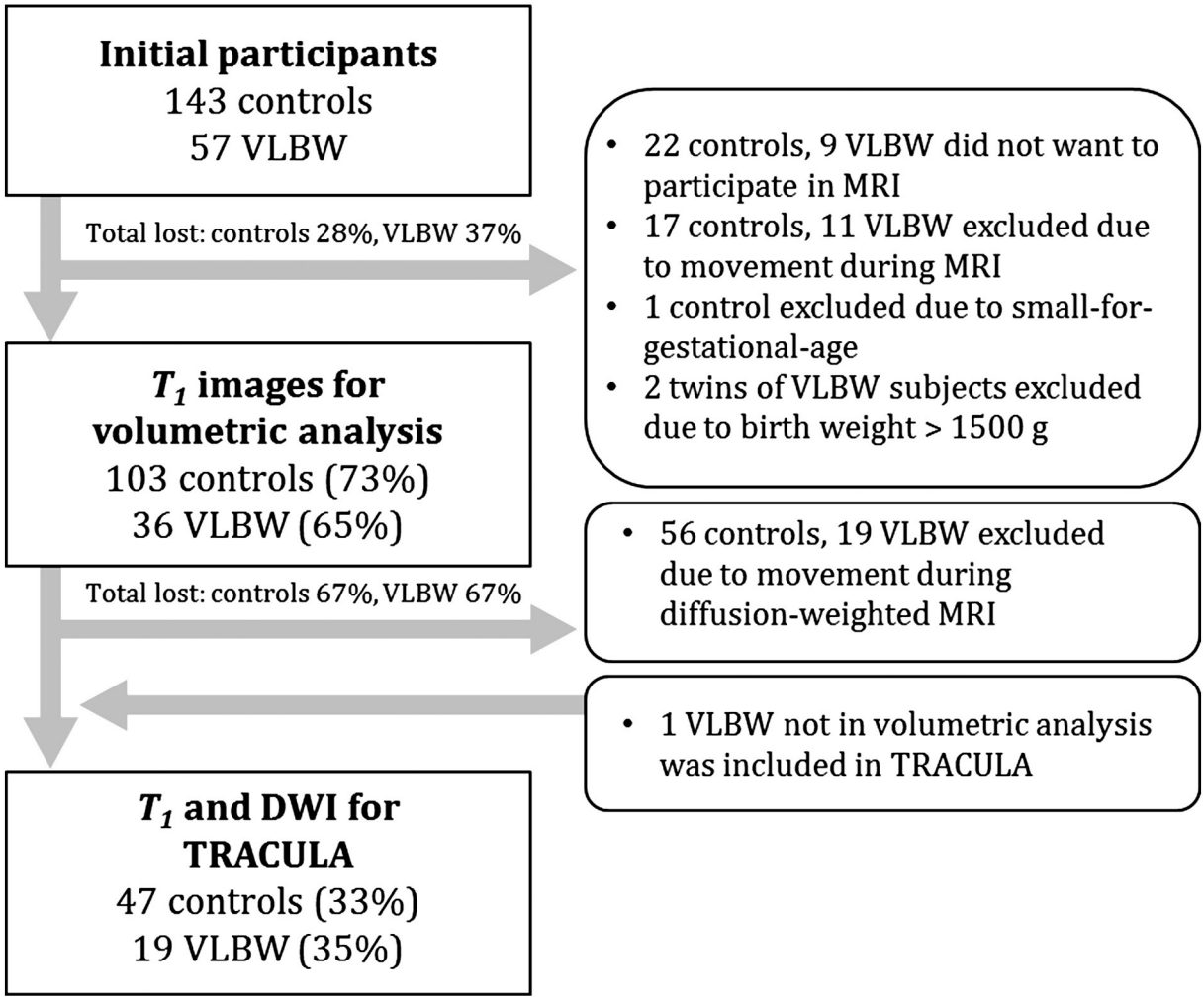

Fig. 1. Overview of participation and retention. Abbreviations: DWI: diffusion-weighted imaging; VLBW: very low birth weight.

7.8 years). Exclusion criteria were severe cerebral palsy (unable to complete neuropsychological testing and MRI), severe sensory impairments, and/or MRI contraindications. One child with retinopathy of prematurity and one with grade 1 intraventricular hemorrhage and mild cerebral palsy who successfully completed the neuropsychological assessments and MRI were included in the analyses. Perinatal health data collected included gestational age, birth weight, Apgar score (at 1 and 5 min), and number of days on mechanical ventilator after birth. Thirty-six VLBW subjects had successful structural MRI and were included in the subcortical volume analysis, and 19 with high-quality diffusion data were included in the dMRI analysis.

Control subjects

The control subjects were recruited from the national Norwegian Mother and Child Cohort Study, managed by the Norwegian Institute of Public Health (Magnus et al., 2006), and born between 2001 and 2007. Age ranged from 5.3 to 10.7 years old (mean age = 8.3 years). Control participants were living in the same geographical area as the VLBW participants and had normal/corrected vision and hearing. Exclusion criteria were current psychiatric treatment, use of psychoactive drugs known to affect central nervous system functioning, birth weight below 2500 g, and/or MRI contraindications. Subcortical volume analysis included 103 control subjects, and 47 controls were included in the dMRI analysis based on quality of their diffusion data (Fig. 1).

Cognitive measures

VLBW subjects were assessed with complete versions of age-appropriate standardized Wechsler intelligence tests: Wechsler Preschool and Primary Scale of Intelligence, 3rd edition (WPPSI-III) (Wechsler, 2002) or Wechsler Intelligence Scale for Children, 4th edition (WISC-IV) (Wechsler, 2003). Controls were assessed with short forms of the corresponding age-appropriate tests: WPSSI-III (four subtests) or Wechsler Abbreviated Scale of Intelligence (WASI) (Wechsler, 1999). Full-scale IQ scores were used for analysis. At neuropsychological assessment, parents reported whether children had received or planned to receive extra help, such as aid of an assistant or help with specific subjects, at school/preschool.

Socio economic status

Hollingshead's (1957) two factor index of social position based on education and occupation of one parent or the mean index of both was used to calculate socioeconomic status.

MRI

MRI data were collected using a 12-channel head coil on a 1.5 T Siemens Avanto scanner (Siemens, Erlangen, Germany). The total scan time was on average 30 min. The pulse sequence used for morphometric analyses was a 3D T_1-weighted magnetization prepared rapid acquisition gradient echo (MPRAGE) scan with the following parameters: TR = 2400 ms, TE = 3.61 ms, TI = 1000 ms; flip angle 8°, FOV 240 × 240 mm^2, and TA = 4 min and 18 min. Each volume consisted of 160 sagittal slices with voxel sizes of 1.25 × 1.25 × 1.20 mm^3.

dMRI was acquired using a conventional 2D single shot balanced-echo EPI sequence. The series acquired diffusion weighting along 30 non-collinear directions (b = 700 s/mm^2), and with 6 images acquired without diffusion weighting (b = 0). The acquisition parameters were: TR = 7700 ms, TE = 70 ms, FOV 256 × 256 mm^2, matrix size 128 × 128, TA = 4:22, BW = 1396 Hz/px, and GRAPPA acceleration factor 2, slice thickness 2 mm. Number of slices was 64 (no gap), with isotropic voxels of 2 × 2 × 2 mm^3.

Each MPRAGE series and the dMRI data were visually inspected, and only scans with no or minimal movement artifacts were included in the analyses. Calculation of head motion during dMRI was done as a part of the TRACULA quality control processing (Yendiki et al., 2013).

Image analysis

All image analysis, including subcortical volumetric segmentation and dMRI analysis, was performed with the freely available FreeSurfer image analysis suite version 5.3.0 (http://surfer.nmr.mgh.harvard.edu). The technical details of the FreeSurfer image processing procedures are described in prior publications (Dale et al., 1999; Dale and Sereno, 1993; Fischl and Dale, 2000; Fischl et al., 2001; Fischl et al., 2002; Fischl et al., 2004a; Fischl et al., 1999a; Fischl et al., 1999b; Fischl et al., 2004b; Han et al., 2006; Jovicich et al., 2006; Ségonne et al., 2004). The subcortical volumetric analysis was based on MRI from 37 VLBW children and 103 controls. The subcortical brain structures included in the analyses (see Table 2) were based on the automated segmentation and labeling procedure in FreeSurfer (Fischl et al., 2002, 2004a), and each structure's volumes from both hemispheres were combined to generate a bilateral volume value. For subcortical volumes, analyses were controlled for estimated total intracranial volume (Buckner et al., 2004).

TRACULA

TRACULA (TRActs Constrained by UnderLying Anatomy), as implemented in FreeSurfer 5.3.0, was used for dMRI analysis and tractography (Yendiki et al., 2011). Briefly, TRACULA applies probabilistic tractography to diffusion data using an anatomical atlas of white matter tracts as well as the subcortical segmentation labels from FreeSurfer (Fischl et al., 2002, 2004a). TRACULA contains an algorithm for automated global probabilistic tractography that estimates the posterior probability of 18 pathways, based on a "ball-and-stick" model of diffusion (Behrens et al., 2007) as well as a pathway prior term, which incorporates prior anatomical knowledge on the pathways from a set of healthy adult training subjects. The prior term expresses the probability of each pathway to pass through, or lie adjacent to, each anatomical segmentation label, calculated separately for every point along the pathway's trajectory. The anatomical segmentation labels come from the cortical parcellation and subcortical segmentation of T_1-weighted MPRAGE images in FreeSurfer. Nineteen VLBW children and 47 controls were included in the TRACULA analyses based on quality of diffusion data. One subject was missing data for forceps major, right corticospinal tract, and right cingulate gyrus, but the remaining values were used for group-level analysis. Eighteen of 19 subjects from the dMRI analysis were also included in the subcortical volume analysis, while one VLBW subject with too poor subcortical data to be analyzed in the volume analysis could be included in TRACULA (see Fig. 1).

Fractional anisotropy (FA), mean diffusivity (MD), radial diffusivity (RD), and axial diffusivity (AD) were assessed in the 18 white matter pathways reconstructed by TRACULA (see Fig. 2): anterior thalamic radiation (ATR) left and right, cingulum–angular (infracallosal) bundle (CAB) left and right, cingulum–cingulate gyrus, (supracallosal) bundle (CCG) left and right, corticospinal tract (CST) left and right, corpus callosum forceps major, corpus callosum forceps minor, inferior longitudinal fasciculus (ILF) left and right, superior longitudinal fasciculus–parietal bundle (SLFP) left and right, superior longitudinal fasciculus–temporal bundle (SLFT, also called arcuate fasciculus) left and right, and uncinate fasciculus (UNC) left and right.

Tract endpoint cortical thickness analysis

In order to explore the relationship between white matter tracts and cortical thickness, we projected the endpoints of the various tracts onto the cortical surface to assess the correlations between dMRI measures from those tracts and the corresponding patch of cortical thickness in the subjects' native space. We obtained regions of interest for the endings of the 18 pathways on the cortical surface by mapping the probability distribution of each of the two end regions of each pathway, as computed by TRACULA, from its native diffusion-weighted imaging (DWI) space to the space of the same subject's T_1-weighted image. We projected the tract endpoints onto the gray/white matter surface by sampling along the surface normal vector, anywhere within 6 mm

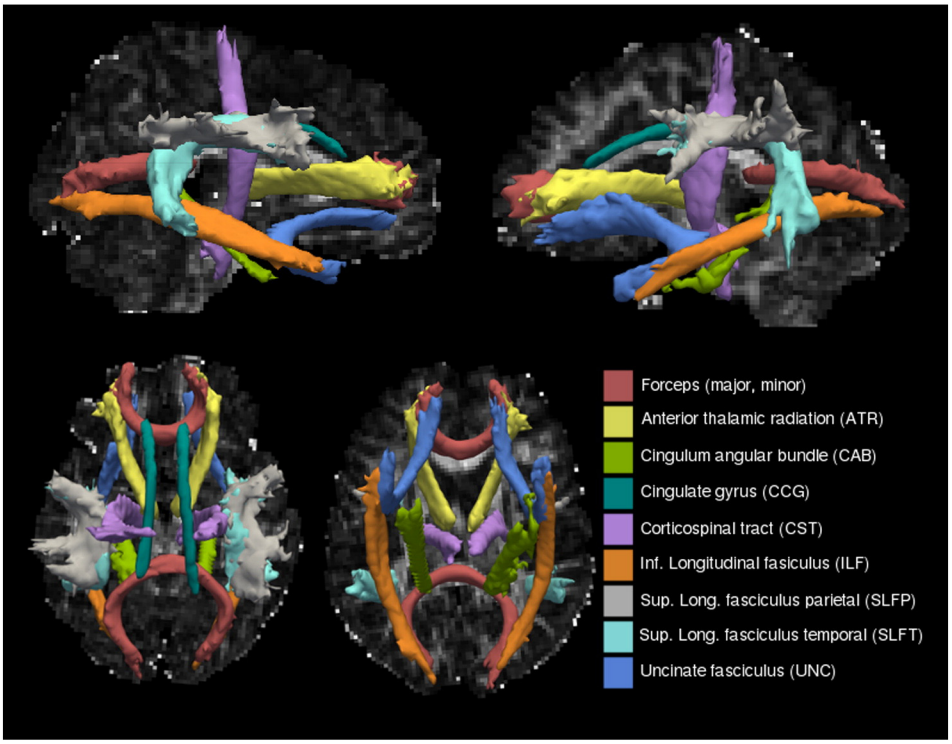

Fig. 2. Probabilistic reconstruction of 18 white matter tracts generated by TRACULA, illustrated here in a control subject.

(3 DWI-space voxels) of the gray/white junction, and then smoothing along the surface with a 2D Gaussian kernel of 6 mm full width at half max.

Tractography pointwise analysis

TRACULA estimates the posterior probability distribution of each pathway in the native DWI space of each subject and finds the maximum probability path, which is a 1D curve in that space. It then calculates the expected value of FA, MD, RD, or AD as a function of position along the pathway by performing a weighted average of the values of each of these four measures at each cross-section of the pathway. These cross-sections are defined at each voxel along the maximum probability path. This yields a 1D sequence of values for each of the four measures, computed in the native space of each subject. These sequences can be used for pointwise analyses of each measure along the trajectory of a pathway.

In order to control the false positive rate, we have chosen to report findings only if they showed significant group differences ($p < 0.05$) over a contiguous segment of length greater than 2 cm along a given pathway.

Statistical analysis

Matlab software suite 2011b (MATLAB and Statistics Toolbox Release 2011b. The MathWorks, Inc., Natick, Massachusetts, USA) was used for statistical analyses of subcortical and cortical morphometry and dMRI data. The software package IBM SPSS 21 (Chicago, USA) was used to generate group difference values and correlations between morphometric, dMRI, IQ, and clinical measures. General linear models were fitted for group comparisons of subcortical brain structure volumes and dMRI data, controlled for age at scan, sex, and IQ; subcortical volume analyses were additionally controlled for estimated total intracranial volume as computed by FreeSurfer. Partial correlation tests, controlled for age at scan and sex, were used to investigate the relationships between morphometry and dMRI and IQ and perinatal data. Data with non-equal variances were analyzed with non-parametric tests and Spearman's ρ. Group analysis for categorical data were tested for significance using Fisher's exact test. Tests for group × age interaction effects were performed for all subcortical structures and for FA, MD, RD, and AD in the white matter tracts. Holm–Bonferroni step-down (Holm, 1979) was used to correct for multiple comparisons for all tests of group differences and correlations.

Ethics

The Regional Committee for Medical Research Ethics approved the study protocol (project number: 2010/2359), and written, informed consent was obtained from the parents/guardians of all participants.

Results

Clinical and cognitive results

Clinical characteristics and full-scale IQ scores are presented in Table 1a and b. VLBW subjects were approximately 6 months younger than control subjects (7.7 vs 8.3 years) in the subcortical sample, while the groups had mean ages of 8.5 and 8.7 years, respectively, in the TRACULA sample. Additional perinatal characteristics for the VLBW group are presented in Table S1.

Full-scale IQ scores were significantly lower in the VLBW group than in controls by approximately 1 standard deviation from control mean, both in the subcortical volume analysis (99 vs 108) and in the dMRI analysis (97 vs 112). IQ scores were still significantly lower in the VLBW group after additionally controlling for socioeconomic status ($p < 0.001$). Controls in the TRACULA analysis had slightly higher IQ scores (4.0 points) than controls in the subcortical volume analysis, but VLBW IQ scores were similar between the analyses. The VLBW group received more help in school and preschool than controls ($p < 0.0001$). The control group had slightly higher average socioeconomic score than the VLBW group.

Subcortical volumes

Compared to controls and after controlling for age, sex, and estimated total intracranial volume, the VLBW group had significantly reduced volumes of thalamus, globus pallidus, hippocampus, cerebral white

Table 1
Overview of major clinical variables and full IQ scores in control and VLBW groups, shown for both (a) subcortical and (b) dMRI analyses.

1a. Subcortical analysis	VLBW (n = 36)			Control (n = 103)			*p*-value
	Mean	SD	Range	Mean	SD	Range	
Birth weight, grams	1019	361	416–1495	3661	485	2510–4950	<0.0001
Gestational age, weeks (days)	29 (0)	2 (6)	23 (4)–35 (1)	Term-born			–
Age at MRI, years	7.8	1.7	5.0–10.5	8.3	1.0	5.3–10.7	0.04
Full-scale IQ	99	9.9	82–132	108	13.6	73–139	<0.001
Socioeconomic status (n = 34, 84)	3.9	0.9	1–5	4.3	0.8	2–5	0.03
Sex: male/female	16/20			49/54			0.8
Subjects with twin	6			0			<0.0001
Received extra help at school, n (%)	10 (28%)			2 (1.9%)			<0.0001
1b. dMRI analysis	**VLBW (n = 19)**			**Control (n = 47)**			***p*-value**
	Mean	SD	Range	Mean	SD	Range	
Birth weight, grams	1103	365	500–1495	3692	531	2550–4950	<0.0001
Gestational age, weeks (days)	29(4)	3(1)	23(4)–35(1)	Term-born			--
Age at MRI, years	8.5	1.2	5.0–10.5	8.7	0.7	7.5–10.6	0.3
Full-scale IQ	97	8.1	82–117	112	13.7	73–134	<0.0001
Socioeconomic status (n = 18, 39)	4.0	0.9	2–5	4.4	0.8	2–5	0.07
Sex: male/female	9/11			22/25			0.9
Subjects with twin	4			0			0.005
Received extra help at school, n (%)	4 (21)			1 (2.1)			0.1

Displayed with *p*-values based on ANOVA between control and VLBW groups. Abbreviations: SD, standard deviation; VLBW, very low birth weight.

matter, ventral diencephalon, brain stem, and in 4 of 5 corpus callosum subsegmentations (Table 2). The ventricular system, comprising lateral, inferior, third, and fourth ventricles, was larger in VLBW subjects. Fig. 3 illustrates the extent of the volume reductions as a percentage of the control group mean for the brain structures that were significantly smaller in the VLBW group.

Partial correlation analysis examined relationships between subcortical volumes and birth weight, gestational age, and IQ, controlled for age and sex and with Holm–Bonferroni step-down. Among VLBW subjects, corpus callosum posterior subsegmentation volume correlated significantly to gestational age ($R = 0.55$, $p = 0.0007$), and cerebellum white matter volume correlated positively to birth weight ($R = 0.53$, $p = 0.001$). No other correlations to gestational age, birth weight, or IQ in the VLBW group reached significance. In controls, birth weight correlated significantly to volumes of cerebellar white matter ($R = 0.49$, $p < 0.0001$), cerebellar gray matter ($R = 0.36$, $p = 0.0002$) and brain stem ($R = 0.42$, $p < 0.0001$). IQ correlated to volumes of thalamus ($R = 0.37$, $p < 0.0001$), hippocampus ($R = 0.35$, $p < 0.0001$), and cerebral white matter ($R = 0.37$, $p < 0.0001$). In the VLBW group, receiving help at school was correlated negatively with corpus callosum volume ($R = -0.46$, $p = 0.008$, uncorrected), but this relationship was not seen in controls. Correlation in controls between IQ and hippocampus volume was not significant after correction for socioeconomic status, and correlations in both groups were not significant with correction for estimated total intracranial volume. There were no significant group × age interaction effects for subcortical structure volumes.

TRACULA results

Group differences

To assess differences in white matter microstructure between the groups, we compared the VLBW group to the control subjects in terms of FA, MD, RD, and AD in the 18 tracts generated by TRACULA. Means and *p*-values for the dMRI measures for tracts with significant group differences are presented in Table 3.

Table 2
Bilateral subcortical volumes (mm^3) in VLBW and control subjects with *p*-values for group differences.

Structure	VLBW		Control		*p*-value
	mean	95% CI	mean	95% CI	
Amygdala	2840	(2752, 2928)	2858	(2808, 2908)	0.73
Brain stem	17,854	(17,373, 18,333)	18,974	(18,700, 19,247)	0.00015*
Caudate	8099	(7811, 8386)	8128	(7963, 8291)	0.87
Cerebellar cortex	113,842	(110,519, 117,164)	113,978	(112,084, 115,872)	0.95
Cerebellar white matter	23,376	(22,552, 24,200)	24,527	(24,056, 24,996)	0.021
Cerebral white matter	400,892	(392,985, 408,799)	420,230	(415,722, 424,737)	7.5×10^{-5}*
Corpus callosum anterior	759	(719, 798)	806	(784, 828)	0.045
Corpus callosum central	317	(292, 341)	391	(377, 404)	9.4×10^{-7} *
Corpus callosum mid-anterior	349	(324, 373)	404	(390, 418)	0.00029*
Corpus callosum mid-posterior	301	(276, 325)	384	(370, 398)	9.6×10^{-8}*
Corpus callosum posterior	660	(619, 700)	774	(751, 796)	5.1×10^{-6}*
Globus pallidus	3499	(3383, 3614)	3751	(3684, 3816)	0.00040*
Hippocampus	7908	(7694, 8121)	8265	(8143, 8386)	0.0059
Nucleus accumbens	1356	(1293, 1418)	1395	(1359, 1430)	0.30
Putamen	11,722	(11,332, 12,111)	11,966	(11,743, 12,188)	0.30
Thalamus	14,039	(13,739, 14,338)	14,703	(14,532, 14,873)	0.00031*
Ventral diencephalon	6859	(6708, 7009)	7109	(7023, 7194)	0.0062*
Ventricular system	20,766	(18,306, 23,225)	11,932	(10,529, 13,333)	1.7×10^{-8}*

Group differences tested using the general linear model, controlled for age, sex, and estimated total intracranial volume. Holm–Bonferroni step-down used to determine significance threshold; significant results denoted by *. Abbreviations: CI, confidence interval; VLBW, very low birth weight.

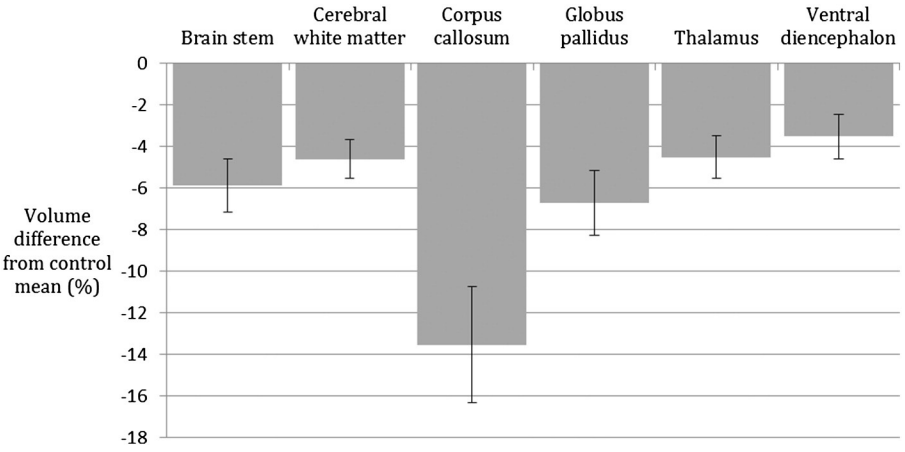

Fig. 3. VLBW subcortical volumes as percentage difference from control mean. Volumes controlled for age, sex, and estimated total intracranial volume. Corpus callosum volume aggregated from all 5 subsegmentations.

No group differences were significant after Holm–Bonferroni step-down, though group differences in several structures were nominally significant at the uncorrected $p < 0.05$ level. The VLBW group showed higher AD in the left SLFP and SLFT, left and right CST, and left CAB. The VLBW group had higher average FA in left CST and in left SLFT. RD was lower in the VLBW group in left CST. Control and VLBW groups did not differ in terms of head motion. There were no correlations after Holm–Bonferroni step-down between dMRI values and subcortical volumes in either group, and there were no significant group × age interaction effects for any of the tracts with nominally significant group differences.

Relationships between dMRI and clinical variables

In relating FA, MD, RD, and AD in all 18 tracts to full-scale IQ, birth weight, and gestational age, we found significant correlations after Holm–Bonferroni step-down in AD in left CAB in the VLBW group with gestational age ($R = 0.86$, $p < 0.0001$). In the control group, birth weight correlated with MD ($R = 0.49$, $p = 0.0009$) and AD ($R = 0.46$, $p = 0.002$) in the right SLFP and AD in the left uncinate fasciculus ($R = 0.52$, $p = 0.0004$). Post-hoc analysis revealed that the number of days VLBW subjects spent on a ventilator after birth correlated negatively with forceps major FA ($R = 0.89$, $p < 0.001$) and positively with forceps major RD ($R = 0.85$, $p < 0.001$), with the five subjects who were on mechanical ventilator in the neonatal period driving the correlations. No other correlations survived Holm–Bonferroni step-down.

Tract endpoint cortical thickness analysis

None of the correlations between dMRI measures and tract endpoint cortical thickness reached significance after Holm–Bonferroni correction for multiple comparisons. However, there were several nominally significant correlations ($p < 0.05$, uncorrected) (Fig. 4). In controls, cortical thickness in the left SLFP parietal endpoint correlated with mean tract MD ($R = 0.30$, $p = 0.046$) and RD ($R = 0.34$, $p = 0.024$), and cortical thickness in the right SLFT temporal endpoint also correlated with mean tract RD ($R = 0.32$, $p = 0.034$). In the VLBW group, right ATR frontal endpoint cortical thickness correlated with mean tract RD ($R = 0.56$, $p = 0.024$); left CCG cortical thickness in the posterior endpoint correlated with mean tract AD ($R = 0.67$, $p = 0.0044$), RD ($R = -0.51$, $p = 0.045$), and FA ($R = 0.61$, $p = 0.0013$); right ILF cortical thickness in the occipital endpoint correlated with mean tract

Table 3
Mean values for FA, MD, RD, and AD in both groups and Cohen's *d* and *p*-values for group differences.

White matter tract	FA				MD [$\times 10^{-4}$ mm^2/s]				RD [$\times 10^{-4}$ mm^2/s]				AD [$\times 10^{-4}$ mm^2/s]			
	VLBW mean	Control mean	d	*p*-value	VLBW mean	Control mean	d	*p*-value	VLBW mean	Control mean	d	*p*-value	VLBW mean	Control mean	d	*p*-value
ATR, left	0.44	0.45	−0.44	0.26	7.9	7.9	0.18	0.67	5.9	5.8	0.31	0.46	12.0	12.0	−0.10	0.82
ATR, right	0.44	0.44	−0.23	0.59	8.0	8.0	0.14	0.74	6.0	5.9	0.08	0.84	12.1	12.1	0.14	0.74
CAB, left	0.35	0.37	−0.78	0.07	8.4	8.5	−0.17	0.68	6.8	6.7	0.29	0.49	11.7	12.0	−1.01	0.018*
CAB, right	0.38	0.39	−0.20	0.63	8.3	8.3	−0.24	0.57	6.5	6.5	−0.02	1.00	11.8	11.9	−0.52	0.22
CCG, left	0.54	0.54	−0.05	0.90	7.8	7.7	0.44	0.29	5.3	5.1	0.35	0.40	12.9	12.8	0.18	0.67
CCG, right	0.47	0.47	0.03	0.92	7.8	7.8	0.19	0.64	5.6	5.6	0.10	0.81	12.1	12.0	0.14	0.73
CST, left	0.58	0.56	1.03	0.015*	7.9	7.9	−0.41	0.33	4.9	5.1	−1.00	0.018*	13.8	13.6	0.86	0.042*
CST, right	0.56	0.55	0.42	0.29	8.0	7.9	0.36	0.39	5.1	5.2	−0.19	0.65	13.7	13.5	0.85	0.045*
Forceps major	0.62	0.63	−0.25	0.55	8.2	8.2	0.09	0.83	4.8	4.7	0.24	0.56	15.0	15.1	−0.31	0.46
Forceps minor	0.59	0.61	−0.58	0.17	8.1	8.0	0.43	0.30	5.0	4.8	0.59	0.16	14.4	14.5	−0.27	0.51
ILF, left	0.52	0.51	0.23	0.57	8.4	8.4	−0.26	0.54	5.8	5.8	−0.24	0.56	13.6	13.7	−0.10	0.81
ILF, right	0.53	0.52	0.46	0.27	8.4	8.5	−0.29	0.49	5.7	5.8	−0.40	0.34	13.9	13.8	0.14	0.73
SLFP, left	0.45	0.44	0.44	0.28	7.9	7.8	0.59	0.16	5.9	5.9	0.07	0.87	11.9	11.6	1.17	0.0065*
SLFP, right	0.44	0.43	0.30	0.42	8.1	8.0	0.46	0.28	6.1	6.0	0.10	0.81	12.0	11.8	0.71	0.09
SLFT, left	0.49	0.47	0.93	0.034*	8.0	7.9	0.25	0.54	5.7	5.8	−0.32	0.45	12.5	12.2	1.23	0.0043*
SLFT, right	0.46	0.45	0.27	0.49	8.0	8.0	−0.04	1.00	5.9	6.0	−0.21	0.61	12.3	12.2	0.26	0.53
UNC, left	0.43	0.43	0.08	0.85	8.3	8.3	−0.10	0.82	6.3	6.3	−0.08	0.85	12.4	12.4	−0.05	0.90
UNC, right	0.45	0.46	−0.48	0.25	8.2	8.2	0.11	0.79	6.1	6.0	0.35	0.40	12.5	12.6	−0.37	0.37

* Denotes nominally significant (uncorrected) at the $p < 0.05$ level. Abbreviations: *d*, Cohen's *d*; AD, axial diffusivity; FA, fractional anisotropy; MD, mean diffusivity; RD, radial diffusivity; CST, corticospinal tract; ILF, inferior longitudinal fasciculus; UNC, uncinate fasciculus; ATR, anterior thalamic radiation; CCG, cingulum–cingulate gyrus bundle; CAB, cingulum–angular bundle; SLFP, superior longitudinal fasciculus–parietal bundle; SLFT, superior longitudinal fasciculus–temporal bundle; VLBW, very low birth weight.

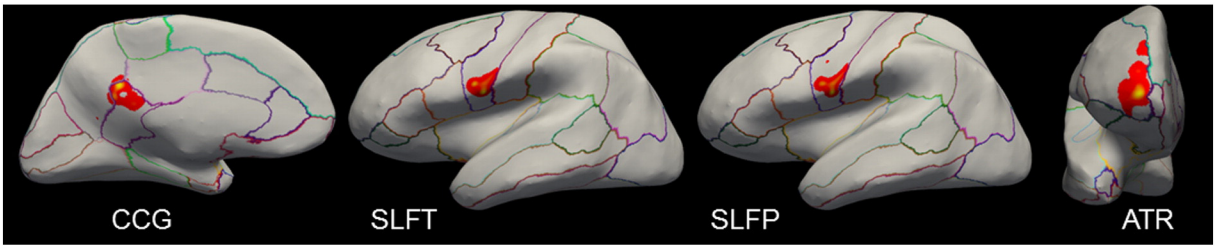

Fig. 4. Examples of projections of left CCG posterior endpoints, left SLFT frontal endpoints, left SLFP frontal endpoints, and right ATR frontal endpoints onto inflated cortical surface, illustrated in a control subject. The red–yellow overlays are the probability distributions of the position of the endings of the corresponding pathways on the surface. Cortical parcellations are outlined based on the Desikan–Killiany atlas (Desikan et al., 2006). Abbreviations: ATR, anterior thalamic radiation, CCG, cingulum cingulate gyrus; SLFP, superior longitudinal fasciculus–parietal bundle; SLFT, superior longitudinal fasciculus–temporal bundle.

MD ($R = 0.62$, $p = 0.011$) and RD ($R = 0.54$, $p = 0.030$); left SLFT cortical thickness in the frontal endpoint correlated with mean tract MD ($R = 0.64$, $p = 0.0076$) and RD ($R = 0.53$, $p = 0.036$); and cortical thickness in the left UNC orbitofrontal endpoint correlated with mean tract MD ($R = 0.57$, $p = 0.021$), RD ($R = 0.79$, $p = 0.00026$), and FA ($R = -0.76$, $p = 0.0007$). Group differences in cortical thickness based on the 34 anatomical regions for each brain hemisphere defined in FreeSurfer were previously reported by Sølsnes et al. (2015).

CCG posterior endpoints were primarily in the isthmus cingulate cortex, and to a lesser extent in adjacent posterior cingulate and precuneus. SLFT and SLFP frontal cortex endpoints were primarily in the precentral gyrus and to a very limited extent in nearby pars opercularis. Cortical ATR endpoints were found in the rostral middle frontal gyrus.

Tractography pointwise analysis

To better localize affected white matter along the various tracts, we conducted a pointwise analysis to identify tract segments with significant group differences ($p < 0.05$) contiguously along at least 2 cm of the tract. The forceps minor showed lower FA and higher RD in the VLBW group along a medial segment of the tract. Left SLFT along the middle of the tract showed higher AD in the VLBW group, which drove the nominally significant group differences in that tract. Additionally, AD in the VLBW group was also higher in two sections of the middle of the right SLFT but did not reach the 2 cm significance threshold.

Discussion

This follow-up study of school-aged children born in the 2000s, comparing those born preterm with VLBW and a term-born control group, found smaller volumes of thalamus, globus pallidus, hippocampus, cerebral white matter, ventral diencephalon, brain stem, and corpus callosum, along with an enlarged ventricular system, in the VLBW group. VLBW subjects had lower FA in a medial segment of forceps minor and higher AD in the middle of the left SLFT, but dMRI measures did not differ significantly between groups at the whole-tract level. Gestational age and birth weight in the VLBW group were generally not associated with subcortical volumes, and IQ did not correlate with either subcortical volumes or dMRI measures in the VLBW group.

Subcortical structure volumes

We found smaller subcortical volumes and larger ventricles in the VLBW group compared to controls, in agreement with earlier reports (Miller et al., 2005; Inder et al., 2003). The VLBW children had reduced volumes of subcortical gray matter, such as thalamus and globus pallidus, and of cerebral white matter including corpus callosum. The increase in ventricular size in preterms is likely due to perinatal deep white matter loss influencing the volume and microstructural characteristics of central white matter tracts (Volpe, 2009; Verney et al., 2012; Judas et al., 2005). Abnormal thalamus microstructure and smaller thalamus (Nagasunder et al., 2011), hippocampus (Aanes et al., 2015), globus pallidus (Lax et al., 2013), and cerebral white matter (Taylor et al., 2011) have been reported in the preterm-born population and may reflect neuron loss and injury to myelinated axons. At their young adulthood follow-up (Bjuland et al., 2014), our older study cohort born in 1986–1988 also showed significant volume reductions in thalamus, cerebral white matter, and the posterior parts of corpus callosum, similar to the findings presented here. This similarity may reflect the influence of *in utero* developmental processes, such as intrauterine growth restriction, on subcortical structures, with consequences for postnatal brain growth.

A complex constellation of neuropathological factors influences brain and cognitive development among preterm VLBW individuals through encephalopathy of prematurity (Volpe, 2009), affecting both gray and white matter. Boardman et al. (2010) described a "common neonatal image phenotype" among children born preterm, consisting of diffuse white matter injury and tissue loss localized to the dorsomedial nucleus of the thalamus, globus pallidus, white matter of the corona radiata, posterior periventricular white matter, and the central region of the centrum semiovale. Moreover, this abnormal phenotype was associated at 2 years of age with reduced developmental quotient, suggesting that the influence of white matter injury on the development of basal ganglia and thalami could have functional consequences (Boardman et al., 2010). Our findings related to lower IQ and greater need for help at school are consistent with this model of restricted growth of the preterm brain in terms of impacts on subcortical volumes and long-term functional deficits. We speculate that this persistent postnatal growth restriction of the brain may be due to a continuation of mechanisms causing intrauterine growth failure, in line with previous studies showing a relationship between lower IQ scores in young adults born small for gestational age with intrauterine growth restriction (Løhaugen et al., 2013; Østgård et al., 2014).

dMRI findings

In contrast to previous reports, the VLBW and control groups had similar FA, MD, AD, and RD values in the 18 white matter tracts assessed in this study. Group differences were only nominally significant and limited to left SLFT (for FA and AD), left SLFP (for AD), left CST (for FA and AD), right CST (for AD), and left CAB (for AD). We previously described (Sølsnes et al., 2015) in an overlapping group from the same cohort significant surface area reductions among VLBW children in the left precentral gyrus, where we found a portion of the SLFP to terminate. Cortical thickness in the white matter tract endpoints demonstrated nominally significant correlations to dMRI values in several regions in frontal, temporal, parietal, and occipital lobes. Our previous report (Sølsnes et al., 2015) found significant differences in surface area and cortical thickness between the VLBW and control groups in the several of the same regions implicated in our cortical endpoint analysis.

Using pointwise analysis, we also identified specific segments of white matter tracts in the forceps minor and SLFT that showed greatest differences between groups on diffusivity measures. While the clinical significance remains to be established, these findings may indicate the localization of the initial perinatal brain injury or delayed myelination.

Changes in FA and diffusivity in superior longitudinal fasciculus (SLF) among individuals born preterm have been frequently reported during infancy, childhood, adolescence, and adulthood (Skranes et al., 2007; Pandit et al., 2013). The SLFT, which corresponds to the arcuate fasciculus, links Wernicke's and Broca's areas (Catani et al., 2002), and the SLFP connects parietal cortex and ventral premotor cortex, including posterior Broca's area (Rushworth et al., 2014). SLFT has been linked to phonological awareness and reading skills in children (Saygin et al., 2013; Yeatman et al., 2011), and both SLFT and SLFP have been hypothesized to be involved in mathematical processing (Jolles et al., 2015). Myall et al. (2013) described possible axonal straightening and increased axonal density in the SLFT, among other tracts, in case studies of adolescents born preterm with ventricular dilation. In our cohort, AD differences in the VLBW group in these long-range association tracts were still evident at early school age. AD and RD have been interpreted in various ways in the neuroimaging literature, including as signifiers of axonal injury and myelin loss (Song et al., 2002), though cautious interpretation of AD and RD is advised especially in clinical populations (Wheeler-Kingshott and Cercignani, 2009).

Similar to our findings, several other studies have also reported very limited difference in FA in preterms compared to controls in childhood (Feldman et al., 2012), adolescence (Frye et al., 2010), and adulthood (Kontis et al., 2009). Thompson et al. (2014) found global increases in MD, RD, and AD in a very preterm group compared to full-term infants, while FA was similar across the groups. Taylor et al. (2011) showed that both structural abnormalities and neuropsychological deficits were more pronounced in VLBW adolescents who were at higher neonatal risk based on birth weight, small for gestational age, severe abnormality on cranial ultrasound, or chronic lung disease, and FA has recently been more associated with complications of preterm birth than with extreme preterm birth in itself (Bonifacio et al., 2010).

In general, the limited dMRI pathology observed here in the VLBW group was somewhat surprising based on previous reports of widespread differences between preterms and controls in white matter tracts among children (Nagy et al., 2003), adolescents (Skranes et al., 2007; Mullen et al., 2011), and young adults (Allin et al., 2011; Eikenes et al., 2011). Although total brain growth is affected in this cohort, with smaller volumes, reduced surface area, and signs of possible cortical reorganization with frontal and occipital thickening (Sølsnes et al., 2015), diffusion measures in the preterm-born children appear similar to their peers born at term. We speculate that perinatal morbidity especially influences white matter development, and that the less severe perinatal morbidity seen in the more recent VLBW cohorts has resulted in fewer deviations in the microstructure of the remaining white matter (Favrais et al., 2014; Gagliardi et al., 2009).

Associations with cognitive performance

Our VLBW group generally scored within the normal IQ range, which was higher than previous study cohorts (Løhaugen et al., 2010). We did not find any relationship between IQ scores and dMRI findings in this study, although diffusion properties in white matter tracts among VLBW individuals have previously been linked to diverse cognitive deficits, ranging from IQ scores (Yung et al., 2007; Eikenes et al., 2011), language skills (Mullen et al., 2011), learning and memory (Salvan et al., 2014), to visual-motor function (Sripada et al., 2015). Significantly more VLBW children in our study received extra help at school or preschool compared to controls ($p < 0.0001$), indicating affected cognitive abilities. Muetzel et al. (2015) showed that white matter microstructure was associated with visual–spatial ability independent of general intelligence in a large sample (n = 778) of normally developing children at 6 to 10 years of age. It is also possible that VLBW individuals exhibit plasticity to develop different neural network trajectories and compensatory connections related to certain cognitive functions (Mürner-Lavanchy et al., 2014; Gozzo et al., 2009; Narberhaus et al., 2009; Van Braeckel et al., 2010; Ment et al., 2009). Focusing on visual–spatial skills, working memory, motor skills, or language-specific tasks, rather than general intelligence, may have detected additional structure-function relationships in our study sample.

Several of the subcortical structures implicated in our group differences analysis are involved in working memory networks. McNab and Klingberg (2008) identify the globus pallidus as essential for controlling access to working memory, while functional and structural imaging of basal ganglia and thalamus have recently shown promise in predicting healthy children's visuospatial working memory two years later (Ullman et al., 2014).

In our cohort born in the late 1980s, Bjuland et al. (2014) found that in VLBW young adults (mean IQ = 89) subcortical volumes correlated strongly with cognitive performance on full-scale IQ. Subcortical volumes in that VLBW group were also strongly associated with birth weight and days in the neonatal intensive care unit. The current study identified volume reductions in nearly all the same subcortical structures, yet the close relationship in the VLBW group to IQ was not apparent. An explanation for this lack of relationship may be the moderate sample size and normal mean IQ scores in the VLBW group.

In Norway, high-risk preterm infants and their families are entitled to special follow-up developmental health services. A quarter of our VLBW participants have had extra help in school or preschool, compared to only 2% of controls. It is plausible that the normal mean IQ score and connectivity in our VLBW group, compared to previous cohorts, reflect in part the availability of such higher-quality educational interventions, although the mean IQ score among VLBW children is still approximately one standard deviation lower than mean IQ in controls. As training and cognitive interventions have been shown to affect white matter (Scholz et al., 2009; Sampaio-Baptista et al., 2013; Hu et al., 2011), it would be worthwhile to explore the direct impact of the combination of advanced medical care and childhood follow-up services on white matter development and connectivity in the high-risk preterm-born population.

Strengths and limitations

The results presented here will provide a useful baseline for follow-up research on these VLBW and term-born cohorts. All subjects underwent structural MRI and dMRI on the same scanner with standardized sequences and were assessed with age-appropriate, standardized cognitive tests. We used TRACULA for reconstruction of major white matter tracts in subjects' native spaces and were able to combine cortical thickness and dMRI data to investigate possible impacts at the transition between white and gray matter. TRACULA's automated reconstruction is based on healthy adult training subjects but has also been used in pediatric populations (Yendiki et al., 2013; Saygin et al., 2013; Koldewyn et al., 2014). The validity of the anatomical data processing stream used in TRACULA for automated surface reconstruction and segmentation of structural images and its lack of age-related bias have been shown previously for children aged 4 to 7 (Ghosh, et al., 2010).

TRACULA includes corpus callosum forceps major and minor, but full corpus callosum segmentation is not available in the current version. Corpus callosum has been implicated in previous studies of VLBW children showing deficits in diverse cognitive skills and would have been an important complement to the 18 tracts described here. Corpus callosum volume, however, is included in our subcortical analysis. While diffusion values for group differences were taken across the entire tract, we examined pointwise to better localize affected white matter segments. Moreover, we chose to control for age and sex; however, larger studies

have shown associations between certain subcortical volumes and age and sex (Koolschijn and Crone, 2013). However, this was a cross-sectional study not intended to identify specific developmental changes within this age range, and the study sample was too small to investigate sex differences within groups.

DWI is very sensitive to motion inside the scanner, which poses a challenge especially for pediatric research. Due to movement artifacts in both groups, the sample available in the TRACULA analysis was about 47% the size of the sample used for subcortical volume analysis. Moreover, a recent estimate suggests that up to 60–90% of all white matter voxels contain multiple fiber orientations (Jeurissen et al., 2013). High-angular resolution diffusion imaging (HARDI) and diffusion spectrum imaging (DSI) are more sensitive than diffusion tensor imaging (DTI) for investigating fiber orientations in areas with crossing fibers (Abhinav et al., 2014; Groeschel et al., 2014) but require longer scan times to measure more diffusion directions, which increases the risk of data loss due to movement artifacts, especially in children. DWI parameters for this study were designed to reduce scan time to accommodate our young subjects and also to improve compatibility with scans from other cohorts. TRACULA does not rely on tensors for tractography but instead uses a crossing-fiber model.

Subjects in the TRACULA sample were on average 5 to 18 months older than those in the volumetric analysis, probably due to more movement in the younger children. VLBW subjects had lower mean socioeconomic status, although very few children in the study had low socioeconomic status, and compared to controls the VLBW group still had significantly lower IQ scores after correction for socioeconomic status.

Conclusion

Consistent with previous reports, this study found significantly reduced volumes of gray and white matter structures including thalamus, globus pallidus, cerebral white matter, and corpus callosum, along with enlarged ventricles in the school-aged VLBW group. By contrast, group differences in dMRI measures were minor and mostly seen in higher AD in the preterm group. In addition, white matter tracts connected to brain regions with cortical deviations showed some evidence of abnormal diffusion measures. This VLBW cohort born in the 2000s showed subcortical volume deviations consistent with previous reports, while white matter connectivity seemed similar between the groups, potentially reflecting different mechanisms on gray and white matter during pre- and postnatal development.

Supplementary data to this article can be found online at http://dx.doi.org/10.1016/j.neuroimage.2015.12.029.

Acknowledgements

We are grateful for the continued participation and cooperation of the families in our study. We thank radiologist Jana Rydland for evaluating the MRI scans clinically, radiographer Bjarte Dagfinn Snekvik for coordinating the imaging, and research assistants Irén Aina Bastholm and Elisabeth Mellemstrand Stavnes. We appreciate the collaboration with Profs. Kristine B. Walhovd and Anders M. Fjell of the Lifespan Changes in Brain and Cognition group, Department of Psychology, University of Oslo, Norway. The Abel Cluster, owned by the University of Oslo and the Norwegian Metacenter for Computational Science and operated by the Department for Research Computing at the University of Oslo Center for Information Technology (http://www.hpc.uio.no), was used for image processing. This project was supported by the Research Council of Norway's FRIMED program (project number 204935/F20) and the Liaison Committee between the Central Norway Regional Health Authority and the Norwegian University of Science and Technology (project number 46056907).

References

Aanes, S., Bjuland, K.J., Skranes, J., Løhaugen, G.C., 2015. Memory function and hippocampal volumes in preterm born very-low-birth-weight (VLBW) young adults. NeuroImage 105, 76–83 (Jan 15).

Aarnoudse-Moens, C.S., Weisglas-Kuperus, N., van Goudoever, J.B., Oosterlaan, J., 2009. Meta-analysis of neurobehavioral outcomes in very preterm and/or very low birth weight children. Pediatrics 124 (2), 717–728 (Aug).

Abhinav, K., Yeh, F.C., Pathak, S., Suski, V., Lacomis, D., Friedlander, R.M., Fernandez-Miranda, J.C., 2014. Advanced diffusion MRI fiber tracking in neurosurgical and neurodegenerative disorders and neuroanatomical studies: a review. Biochim. Biophys. Acta 1842 (11), 2286–2297 (Nov).

Allin, M.P., Kontis, D., Walshe, M., Wyatt, J., Barker, G.J., Kanaan, R.A., McGuire, P., Rifkin, L., Murray, R.M., Nosarti, C., 2011. White matter and cognition in adults who were born preterm. PLoS ONE 6 (10), e24525.

Back, S.A., Riddle, A., McClure, M.M., 2007. Maturation-dependent vulnerability of perinatal white matter in premature birth. Stroke 38 (Suppl. 2), 724–730 (Review, Feb).

Banker, B.Q., Larroche, J.C., 1962. Periventricular leukomalacia of infancy. A form of neonatal anoxic encephalopathy. Arch. Neurol. 7, 386–410.

Behrens, T.E., Berg, H.J., Jbabdi, S., Rushworth, M.F., Woolrich, M.W., 2007. Probabilistic diffusion tractography with multiple fibre orientations: what can we gain? NeuroImage 34 (1), 144–155 (Jan 1).

Bjuland, K.J., Løhaugen, G.C., Martinussen, M., Skranes, J., 2013. Cortical thickness and cognition in very-low-birth-weight late teenagers. Early Hum. Dev. 89 (6), 371–380 (Jan 1).

Bjuland, K.J., Rimol, L.M., Løhaugen, G.C., Skranes, J., 2014. Brain volumes and cognitive function in very-low-birth-weight (VLBW) young adults. Eur. J. Paediatr. Neurol. 18 (5), 578–590 (Sep).

Boardman, J.P., Counsell, S.J., Rueckert, D., Kapellou, O., Bhatia, K.K., Aljabar, P., Hajnal, J., Allsop, J.M., Rutherford, M.A., Edwards, A.D., 2006. Abnormal deep grey matter development following preterm birth detected using deformation-based morphometry. NeuroImage 32 (1), 70–78 (Aug 1).

Boardman, J.P., Craven, C., Valappil, S., Counsell, S.J., Dyet, L.E., Rueckert, D., Aljabar, P., Rutherford, M.A., Chew, A.T., Allsop, J.M., Cowan, F., Edwards, A.D., 2010. A common neonatal image phenotype predicts adverse neurodevelopmental outcome in children born preterm. NeuroImage 52 (2), 409–414 (Aug 15).

Bonifacio, S.L., Glass, H.C., Chau, V., Berman, J.I., Xu, D., Brant, R., Barkovich, A.J., Poskitt, K.J., Miller, S.P., Ferriero, D.M., 2010. Extreme premature birth is not associated with impaired development of brain microstructure. J. Pediatr. 157 (5), 726–732, e1 (Nov).

Buckner, R.L., Head, D., Parker, J., Fotenos, A.F., Marcus, D., Morris, J.C., Snyder, A.Z., 2004. A unified approach for morphometric and functional data analysis in young, old, and demented adults using automated atlas-based head size normalization: reliability and validation against manual measurement of total intracranial volume. NeuroImage 23 (2), 724–738 (Oct).

Catani, M., Howard, R.J., Pajevic, S., Jones, D.K., 2002. Virtual in vivo interactive dissection of white matter fasciculi in the human brain. NeuroImage 17 (1), 77–94 (Sep).

Chang, H.H., Larson, J., Blencowe, H., Spong, C.Y., Howson, C.P., Cairns-Smith, S., Lackritz, E.M., Lee, S.K., Mason, E., Serazin, A.C., Walani, S., Simpson, J.L., Lawn, J.E., 2013. Born too soon preterm prevention analysis group. Preventing preterm births: analysis of trends and potential reductions with interventions in 39 countries with very high human development index. Lancet 381 (9862), 223–234. http://dx.doi.org/10.1016/S0140-6736(12)61856-X (Epub 2012 Nov 16, Jan 19).

Constable, R.T., Ment, L.R., Vohr, B.R., Kesler, S.R., Fulbright, R.K., Lacadie, C., Delancy, S., Katz, K.H., Schneider, K.C., Schafer, R.J., Makuch, R.W., Reiss, A.R., 2008. Prematurely born children demonstrate white matter microstructural differences at 12 years of age, relative to term control subjects: an investigation of group and gender effects. Pediatrics 121 (2), 306–316 (Feb).

Counsell, S.J., Edwards, A.D., Chew, A.T., Anjari, M., Dyet, L.E., Srinivasan, L., Boardman, J.P., Allsop, J.M., Hajnal, J.V., Rutherford, M.A., Cowan, F.M., 2008. Specific relations between neurodevelopmental abilities and white matter microstructure in children born preterm. Brain 131 (Pt 12), 3201–3208 (Dec).

Dale, A.M., Sereno, M.I., 1993. Improved localizadon of cortical activity by combining EEG and MEG with MRI cortical surface reconstruction: a linear approach. J. Cogn. Neurosci. 5 (2), 162–176 (Spring).

Dale, A.M., Fischl, B., Sereno, M.I., 1999. Cortical surface-based analysis. I. Segmentation and surface reconstruction. NeuroImage 9 (2), 179–194 (Feb).

Desikan, R.S., Ségonne, F., Fischl, B., Quinn, B.T., Dickerson, B.C., Blacker, D., Buckner, R.L., Dale, A.M., Maguire, R.P., Hyman, B.T., Albert, M.S., Killiany, R.J., 2006. An automated labeling system for subdividing the human cerebral cortex on MRI scans into gyral based regions of interest. NeuroImage 31 (3), 968–980 (Jul 1).

Eikenes, L., Løhaugen, G.C., Brubakk, A.M., Skranes, J., Håberg, A.K., 2011. Young adults born preterm with very low birth weight demonstrate widespread white matter alterations on brain DTI. NeuroImage 54 (3), 1774–1785 (Feb 1).

Favrais, G., Tourneux, P., Lopez, E., Durrmeyer, X., Gascoin, G., Ramful, D., Zana-Taieb, E., Baud, O., 2014. Impact of common treatments given in the perinatal period on the developing brain. Neonatology 106 (3), 163–172.

Feldman, H.M., Lee, E.S., Loe, I.M., Yeom, K.W., Grill-Spector, K., Luna, B., 2012. White matter microstructure on diffusion tensor imaging is associated with conventional magnetic resonance imaging findings and cognitive function in adolescents born preterm. Dev. Med. Child Neurol. 54 (9), 809–814 (Sep).

Ferriero, D.M., 2004. Neontal brain injury. N. Engl. J. Med. 351, 1985–1995.

Fischl, B., Dale, A.M., 2000. Measuring the thickness of the human cerebral cortex from magnetic resonance images. Proc. Natl. Acad. Sci. U. S. A. 97 (20), 11050–11055 (Sep 26).

Fischl, B., Sereno, M.I., Dale, A.M., 1999a. Cortical surface-based analysis. II: inflation, flattening, and a surface-based coordinate system. NeuroImage 9 (2), 195–207 (Feb).

Fischl, B., Sereno, M.I., Tootell, R.B., Dale, A.M., 1999b. High-resolution intersubject averaging and a coordinate system for the cortical surface. Hum. Brain Mapp. 8 (4), 272–284.
Fischl, B., Liu, A., Dale, A.M., 2001. Automated manifold surgery: constructing geometrically accurate and topologically correct models of the human cerebral cortex. IEEE Trans. Med. Imaging 20 (1), 70–80 (Jan).
Fischl, B., Salat, D.H., Busa, E., Albert, M., Dieterich, M., Haselgrove, C., van der Kouwe, A., Killiany, R., Kennedy, D., Klaveness, S., Montillo, A., Makris, N., Rosen, B., Dale, A.M., 2002. Whole brain segmentation: automated labeling of neuroanatomical structures in the human brain. Neuron 33 (3), 341–355 (Jan 31).
Fischl, B., Salat, D.H., van der Kouwe, A.J., Makris, N., Ségonne, F., Quinn, B.T., Dale, A.M., 2004a. Sequence-independent segmentation of magnetic resonance images. NeuroImage 23 (Suppl. 1), S69–S84.
Fischl, B., van der Kouwe, A., Destrieux, C., Halgren, E., Ségonne, F., Salat, D.H., Busa, E., Seidman, L.J., Goldstein, J., Kennedy, D., Caviness, V., Makris, N., Rosen, B., Dale, A.M., 2004b. Automatically parcellating the human cerebral cortex. Cereb. Cortex 14 (1), 11–22 (Jan).
Frye, R.E., Hasan, K., Malmberg, B., Desouza, L., Swank, P., Smith, K., Landry, S., 2010. Superior longitudinal fasciculus and cognitive dysfunction in adolescents born preterm and at term. Dev. Med. Child Neurol. 52 (8), 760–766 (Aug).
Gagliardi, L., Bellù, R., Zanini, R., Dammann, O., 2009. Network Neonatale Lombardo Study Group. Bronchopulmonary dysplasia and brain white matter damage in the preterm infant: a complex relationship. Paediatr. Perinat. Epidemiol. 23 (6), 582–590 (Nov).
Ghosh, S.S., Kakunoori, S., Augustinack, J., Nieto-Castanon, A., Kovelman, I., Gaab, N., Christodoulou, J.A., Triantafyllou, C., Gabrieli, J.D., Fischl, B., 2010. Evaluating the validity of volume-based and surface-based brain image registration for developmental cognitive neuroscience studies in children 4 to 11 years of age. NeuroImage 53 (1), 85–93 (Oct 15).
Gozzo, Y., Vohr, B., Lacadie, C., Hampson, M., Katz, K.H., Maller-Kesselman, J., Schneider, K.C., Peterson, B.S., Rajeevan, N., Makuch, R.W., Constable, R.T., Ment, L.R., 2009. Alterations in neural connectivity in preterm children at school age. NeuroImage 48 (2), 458–463 (Nov 1).
Groeschel, S., Tournier, J.D., Northam, G.B., Baldeweg, T., Wyatt, J., Vollmer, B., Connelly, A., 2014. Identification and interpretation of microstructural abnormalities in motor pathways in adolescents born preterm. NeuroImage 87, 209–219 (Feb 15).
Han, X., Jovicich, J., Salat, D., van der Kouwe, A., Quinn, B., Czanner, S., Busa, E., Pacheco, J., Albert, M., Killiany, R., Maguire, P., Rosas, D., Makris, N., Dale, A., Dickerson, B., Fischl, B., 2006. Reliability of MRI-derived measurements of human cerebral cortical thickness: the effects of field strength, scanner upgrade and manufacturer. NeuroImage 32 (1), 180–194 (Aug 1).
Haynes, R.L., Xu, G., Folkerth, R.D., Trachtenberg, F.L., Volpe, J.J., Kinney, H.C., 2011. Potential neuronal repair in cerebral white matter injury in the human neonate. Pediatr. Res. 69 (1), 62–67 (Jan).
Hintz, S.R., O'Shea, M., 2008. Neuroimaging and neurodevelopmental outcomes in preterm infants. Semin. Perinatol. 32 (1), 11–19 (Feb).
Hollingshead, A.B., 1957. Two Factor Index of Social Position. Mimeo. New Haven, Connecticut: Yale University.
Holm, S., 1979. A simple sequentially rejective multiple test procedure. Scand. J. Stat. 6, 65–70.
Hu, Y., Geng, F., Tao, L., Hu, N., Du, F., Fu, K., Chen, F., 2011. Enhanced white matter tracts integrity in children with abacus training. Hum. Brain Mapp. 32 (1), 10–21 (Jan).
Inder, T.E., Anderson, N.J., Spencer, C., Wells, S., Volpe, J.J., 2003. White matter injury in the premature infant: a comparison between serial cranial sonographic and MR findings at term. AJNR Am. J. Neuroradiol. 24 (5), 805–809 (May).
Jeurissen, B., Leemans, A., Tournier, J.D., Jones, D.K., Sijbers, J., 2013. Investigating the prevalence of complex fiber configurations in white matter tissue with diffusion magnetic resonance imaging. Hum. Brain Mapp. 34 (11), 2747–2766 (Nov).
Johansen-Berg, H., Behrens, T.E.J. (Eds.), 2014. Diffusion MRI: From Quantitative Measurement to In-vivo Neuroanatomy, second ed. Academic Press, London.
Jolles, D., Wassermann, D., Chokhani, R., Richardson, J., Tenison, C., Bammer, R., Fuchs, L., Supekar, K., Menon, V., 2015. Plasticity of left perisylvian white-matter tracts is associated with individual differences in math learning. Brain Struct. Funct. (Jan 21).
Jovicich, J., Czanner, S., Greve, D., Haley, E., van der Kouwe, A., Gollub, R., Kennedy, D., Schmitt, F., Brown, G., Macfall, J., Fischl, B., Dale, A., 2006. Reliability in multi-site structural MRI studies: effects of gradient non-linearity correction on phantom and human data. NeuroImage 30 (2), 436–443 (Apr 1).
Judas, M., Rados, M., Jovanov-Milosevic, N., Hrabac, P., Stern-Padovan, R., Kostovic, I., 2005. Structural, immunocytochemical, and MR imaging properties of periventricular crossroads of growing cortical pathways in preterm infants. AJNR Am. J. Neuroradiol. 26 (10), 2671–2684 (Nov-Dec).
Koldewyn, K., Yendiki, A., Weigelt, S., Gweon, H., Julian, J., Richardson, H., Malloy, C., Saxe, R., Fischl, B., Kanwisher, N., 2014. Differences in the right inferior longitudinal fasciculus but no general disruption of white matter tracts in children with autism spectrum disorder. Proc. Natl. Acad. Sci. U. S. A. 111 (5), 1981–1986 (Feb 4).
Kontis, D., Catani, M., Cuddy, M., Walshe, M., Nosarti, C., Jones, D., Wyatt, J., Rifkin, L., Murray, R., Allin, M., 2009. Diffusion tensor MRI of the corpus callosum and cognitive function in adults born preterm. Neuroreport 20 (4), 424–428 (Mar 4).
Koolschijn, P.C., Crone, E.A., 2013. Sex differences and structural brain maturation from childhood to early adulthood. Dev. Cogn. Neurosci. 5, 106–118 (Jul).
Lawn, J.E., Blencowe, H., Oza, S., You, D., Lee, A.C., Waiswa, P., Lalli, M., Bhutta, Z., Barros, A.J., Christian, P., Mathers, C., Cousens, S.N., 2014. Lancet every newborn study group. Every newborn: progress, priorities, and potential beyond survival. Lancet 384 (9938), 189–205 (Jul 12). Erratum in: Lancet. 2014;384(9938):132.
Lax, I.D., Duerden, E.G., Lin, S.Y., Mallar Chakravarty, M., Donner, E.J., Lerch, J.P., Taylor, M.J., 2013. Neuroanatomical consequences of very preterm birth in middle childhood. Brain Struct. Funct. 218 (2), 575–585 (Mar).
Le Bihan, D., Johansen-Berg, H., 2012. Diffusion MRI at 25: exploring brain tissue structure and function. NeuroImage 61 (2), 324–341 (Jun).
Løhaugen, G.C., Gramstad, A., Evensen, K.A., Martinussen, M., Lindqvist, S., Indredavik, M., Vik, T., Brubakk, A.M., Skranes, J., 2010. Cognitive profile in young adults born preterm at very low birthweight. Dev. Med. Child Neurol. 52 (12), 1133–1138 (Dec).
Løhaugen, G.C., Østgård, H.F., Andreassen, S., Jacobsen, G.W., Vik, T., Brubakk, A.M., Skranes, J., Martinussen, M., 2013. Small for gestational age and intrauterine growth restriction decreases cognitive function in young adults. J. Pediatr. 163 (2), 447–453 (Aug).
Lowe, J., Duvall, S.W., MacLean, P.C., Caprihan, A., Ohls, R., Qualls, C., Phillips, J., 2011. Comparison of structural magnetic resonance imaging and development in toddlers born very low birth weight and full-term. J. Child Neurol. 26 (5), 586–592 (May).
Lund, L.K., Vik, T., Lydersen, S., Løhaugen, G.C., Skranes, J., Brubakk, A.M., Indredavik, M.S., 2012. Mental health, quality of life and social relations in young adults born with low birth weight. Health Qual. Life Outcomes 10, 146 (Dec 5).
Magnus, P., Irgens, L.M., Haug, K., Nystad, W., Skjærven, R., Stoltenberg, C., the Cohort Study Group, 2006. Cohort profile: the Norwegian mother and child cohort study (MoBa). Int. J. Epidemiol. 35, 1146–1150.
Martinussen, M., Fischl, B., Larsson, H.B., Skranes, J., Kulseng, S., Vangberg, T.R., Vik, T., Brubakk, A.M., Haraldseth, O., Dale, A.M., 2005. Cerebral cortex thickness in 15-year-old adolescents with low birth weight measured by an automated MRI-based method. Brain 128 (Pt 11), 2588–2596 (Nov).
McNab, F., Klingberg, T., 2008. Prefrontal cortex and basal ganglia control access to working memory. Nat. Neurosci. 11 (1), 103–107 (Jan).
Ment, L.R., Hirtz, D., Hüppi, P.S., 2009. Imaging biomarkers of outcome in the developing preterm brain. Lancet Neurol. 8 (11), 1042–1055 (Nov).
Mento, G., Bisiacchi, P.S., 2012. Neurocognitive development in preterm infants: insights from different approaches. Neurosci. Biobehav. Rev. 36 (1), 536–555 (Jan).
Miller, S.P., Ferriero, D.M., Leonard, C., Piecuch, R., Glidden, D.V., Partridge, J.C., Perez, M., Mukherjee, P., Vigneron, D.B., Barkovich, A.J., 2005. Early brain injury in premature newborns detected with magnetic resonance imaging is associated with adverse early neurodevelopmental outcome. J. Pediatr. 147 (5), 609–616 (Nov).
Muetzel, R.L., Mous, S.E., van der Ende, J., Blanken, L.M., van der Lugt, A., Jaddoe, V.W., Verhulst, F.C., Tiemeier, H., White, T., 2015. White matter integrity and cognitive performance in school-age children: a population-based neuroimaging study. NeuroImage 119, 119–128 (Jun 8).
Mullen, K.M., Vohr, B.R., Katz, K.H., Schneider, K.C., Lacadie, C., Hampson, M., Makuch, R.W., Reiss, A.L., Constable, R.T., Ment, L.R., 2011. Preterm birth results in alterations in neural connectivity at age 16 years. NeuroImage 54 (4), 2563–2570 (Feb 14).
Mürner-Lavanchy, I., Steinlin, M., Kiefer, C., Weisstanner, C., Ritter, B.C., Perrig, W., Everts, R., 2014. Delayed development of neural language organization in very preterm born children. Dev. Neuropsychol. 39 (7), 529–542.
Murray, A.L., Scratch, S.E., Thompson, D.K., Inder, T.E., Doyle, L.W., Anderson, J.F., Anderson, P.J., 2014. Neonatal brain pathology predicts adverse attention and processing speed outcomes in very preterm and/or very low birth weight children. Neuropsychology 28 (4), 552–562 (Jul).
Myall, N.J., Yeom, K.W., Yeatman, J.D., Gaman-Bean, S., Feldman, H.M., 2013. Case series: fractional anisotropy along the trajectory of selected white matter tracts in adolescents born preterm with ventricular dilation. J. Child Neurol. 28 (6), 774–780 (Jun).
Nagasunder, A.C., Kinney, H.C., Blüml, S., Tavaré, C.J., Rosser, T., Gilles, F.H., Nelson, M.D., Panigrahy, A., 2011. Abnormal microstructure of the atrophic thalamus in preterm survivors with periventricular leukomalacia. AJNR Am. J. Neuroradiol. 32 (1), 185–191 (Jan).
Nagy, Z., Westerberg, H., Skare, S., Andersson, J.L., Lilja, A., Flodmark, O., Fernell, E., Holmberg, K., Bohm, B., Forssberg, H., Lagercrantz, H., Klingberg, T., 2003. Preterm children have disturbances of white matter at 11 years of age as shown by diffusion tensor imaging. Pediatr. Res. 54 (5), 672–679 (Nov).
Narberhaus, A., Lawrence, E., Allin, M.P., Walshe, M., McGuire, P., Rifkin, L., Murray, R., Nosarti, C., 2009. Neural substrates of visual paired associates in young adults with a history of very preterm birth: alterations in fronto-parieto-occipital networks and caudate nucleus. NeuroImage 47 (4), 1884–1893 (Oct 1).
Ortinau, C., Neil, J., 2015. The neuroanatomy of prematurity: normal brain development and the impact of preterm birth. Clin. Anat. 28 (2), 168–183 (Mar).
Østgård, H.F., Løhaugen, G.C., Bjuland, K.J., Rimol, L.M., Brubakk, A.M., Martinussen, M., Vik, T., Håberg, A.K., Skranes, J., 2014. Brain morphometry and cognition in young adults born small for gestational age at term. J. Pediatr. 165 (5), 921–927, e1 (Nov).
Pandit, A.S., Ball, G., Edwards, A.D., Counsell, S.J., 2013. Diffusion magnetic resonance imaging in preterm brain injury. Neuroradiology 55 (Suppl. 2), 65–95 (Sep).
Rushworth, M.F.S., Sallet, J., Boorman, E.D., Johansen-Berg, H., TEJ, B., 2014. Mars RB Comparing Connections in the Brains of Humans and Other Primates Using Diffusion-Weighted Imaging. Diffusion MRI, 2nd edition Academic Press, Amsterdam, pp. 569–584 http://dx.doi.org/10.1016/B978-0-12-396460-1.00024-X.
Saigal, S., Doyle, L.W., 2008. An overview of mortality and sequelae of preterm birth from infancy to adulthood. Lancet 371 (9608), 261–269 (Jan 19).
Salvan, P., Froudist Walsh, S., Allin, M.P., Walshe, M., Murray, R.M., Bhattacharyya, S., McGuire, P.K., Williams, S.C., Nosarti, C., 2014. Road work on memory lane—functional and structural alterations to the learning and memory circuit in adults born very preterm. NeuroImage 102 (Pt 1), 152–161 (Nov 15).
Sampaio-Baptista, C., Khrapitchev, A.A., Foxley, S., Schlagheck, T., Scholz, J., Jbabdi, S., DeLuca, G.C., Miller, K.L., Taylor, A., Thomas, N., Kleim, J., Sibson, N.R., Bannerman, D., Johansen-Berg, H., 2013. Motor skill learning induces changes in white matter microstructure and myelination. J. Neurosci. 33 (50), 19499–19503 (Dec 11).
Saygin, Z.M., Norton, E.S., Osher, D.E., Beach, S.D., Cyr, A.B., Ozernov-Palchik, O., Yendiki, A., Fischl, B., Gaab, N., Gabrieli, J.D., 2013. Tracking the roots of reading ability: white matter volume and integrity correlate with phonological awareness in prereading and early-reading kindergarten children. J. Neurosci. 33 (33), 13251–13258 (Aug 14).

Scholz, J., Klein, M.C., Behrens, T.E., Johansen-Berg, H., 2009. Training induces changes in white-matter architecture. Nat. Neurosci. 12 (11), 1370–1371 (Nov).
Ségonne, F., Dale, A.M., Busa, E., Glessner, M., Salat, D., Hahn, H.K., Fischl, B., 2004. A hybrid approach to the skull stripping problem in MRI. NeuroImage 22 (3), 1060–1075 (Jul).
Skranes, J., Vangberg, T.R., Kulseng, S., Indredavik, M.S., Evensen, K.A., Martinussen, M., Dale, A.M., Haraldseth, O., Brubakk, A.M., 2007. Clinical findings and white matter abnormalities seen on diffusion tensor imaging in adolescents with very low birth weight. Brain 130 (Pt 3), 654–666 (Mar).
Skranes, J., Løhaugen, G.C., Martinussen, M., Håberg, A., Brubakk, A.M., Dale, A.M., 2013. Cortical surface area and IQ in very-low-birth-weight (VLBW) young adults. Cortex 49 (8), 2264–2271. http://dx.doi.org/10.1016/j.cortex.2013.06.001 (Sep).
Sølsnes, A.E., Grunewaldt, K.H., Bjuland, K.J., Stavnes, E.M., Bastholm, I.A., Aanes, S., Østgård, H.F., Håberg, A., Løhaugen, G.C., Skranes, J., Rimol, L.M., 2015. Cortical morphometry and IQ in VLBW children without cerebral palsy born in 2003–2007. Neuroimaging Clin. 8, 193–201 (Apr 14).
Song, S.K., Sun, S.W., Ramsbottom, M.J., Chang, C., Russell, J., Cross, A.H., 2002. Dysmyelination revealed through MRI as increased radial (but unchanged axial) diffusion of water. NeuroImage 17 (3), 1429–1436 (Nov).
Sripada, K., Løhaugen, G.C., Eikenes, L., Bjørlykke, K.M., Håberg, A.K., Skranes, J., Rimol, L.M., 2015. Visual-motor deficits relate to altered gray and white matter in young adults born preterm with very low birth weight. NeuroImage 109, 493–504 (Apr 1).
Taylor, H.G., Filipek, P.A., Juranek, J., Bangert, B., Minich, N., Hack, M., 2011. Brain volumes in adolescents with very low birth weight: effects on brain structure and associations with neuropsychological outcomes. Dev. Neuropsychol. 36 (1), 96–117.
Thompson, D.K., Lee, K.J., Egan, G.F., Warfield, S.K., Doyle, L.W., Anderson, P.J., Inder, T.E., 2014. Regional white matter microstructure in very preterm infants: predictors and 7 year outcomes. Cortex 52, 60–74 (Mar).
Ullman, H., Almeida, R., Klingberg, T., 2014. Structural maturation and brain activity predict future working memory capacity during childhood development. J. Neurosci. 34 (5), 1592–1598 (Jan 29).
Van Braeckel, K., Butcher, P.R., Geuze, R.H., van Duijn, M.A., Bos, A.F., Bouma, A., 2010. Difference rather than delay in development of elementary visuomotor processes in children born preterm without cerebral palsy: a quasi-longitudinal study. Neuropsychology 24 (1), 90–100 (Jan).
Verney, C., Pogledic, I., Biran, V., Adle-Biassette, H., Fallet-Bianco, C., Gressens, P., 2012. Microglial reaction in axonal crossroads is a hallmark of noncystic periventricular white matter injury in very preterm infants. J. Neuropathol. Exp. Neurol. 71 (3), 251–264 (Mar).
Volpe, J.J., 2009. Brain injury in premature infants: a complex amalgam of destructive and developmental disturbances. Lancet Neurol. 8 (1), 110–124 (Jan).
Volpe, J.J., Kinney, H.C., Jensen, F.E., Rosenberg, P.A., 2011. The developing oligodendrocyte: key cellular target in brain injury in the premature infant. Int. J. Dev. Neurosci. 29 (4), 423–440 (Jun).
Wechsler, D., 1999. Wechsler Abbreviated Scale of Intelligence. Pearson, San Antonio.
Wechsler, D., 2002. Wechsler Preschool and Primary Scale of Intelligence, Third Edition Norwegian Version. 2008 ed. Pearson, San Antonio.
Wechsler, D., 2003. Wechsler Intelligence Scale for Children, Fourth Edition. Norwegian Version. 2009 ed. Pearson, London.
Wheeler-Kingshott, C.A., Cercignani, M., 2009. About "axial" and "radial" diffusivities. Magn. Reson. Med. 61 (5), 1255–1260 (May).
Wilson-Costello, D., Friedman, H., Minich, N., Fanaroff, A.A., Hack, M., 2005. Improved survival rates with increased neurodevelopmental disability for extremely low birth weight infants in the 1990s. Pediatrics 115 (4), 997–1003 (Apr).
Yeatman, J.D., Dougherty, R.F., Rykhlevskaia, E., Sherbondy, A.J., Deutsch, G.K., Wandell, B.A., Ben-Shachar, M., 2011. Anatomical properties of the arcuate fasciculus predict phonological and reading skills in children. J. Cogn. Neurosci. 23 (11), 3304–3317 (Nov).
Yendiki, A., Panneck, P., Srinivasan, P., Stevens, A., Zöllei, L., Augustinack, J., Wang, R., Salat, D., Ehrlich, S., Behrens, T., Jbabdi, S., Gollub, R., Fischl, B., 2011. Automated probabilistic reconstruction of white-matter pathways in health and disease using an atlas of the underlying anatomy. Front. Neuroinform. 5, 23 (Oct 14).
Yendiki, A., Koldewyn, K., Kakunoori, S., Kanwisher, N., Fischl, B., 2013. Spurious group differences due to head motion in a diffusion MRI study. NeuroImage 88C, 79–90 Nov 21.
Yung, A., Poon, G., Qiu, D.Q., Chu, J., Lam, B., Leung, C., Goh, W., Khong, P.L., 2007. White matter volume and anisotropy in preterm children: a pilot study of neurocognitive correlates. Pediatr. Res. 61 (6), 732–736 (Jun).